RED VARIABLE STARS. II. SPECTRAL CLASSIFICATION OF MIRA VARIABLES WITH PHENOMENOLOGICAL AND PHOTOMETRIC PROCEDURE[a]

L. CELIS S.[b]
Grupo de Astronomía y Astrofísica, Facultad de Física Universidad Católica de Chile, Casilla 114-D, Santiago, Chile
Received 24 May 1983; revised 14 November 1983

ABSTRACT

The spectral classification provided in the present work is based on 167 spectrograms obtained at the Cerro Tololo Inter-American Observatory, for 28 Mira variables. A selection of spectrographic profiles is made of the M0 to M8 classification. A *UBVRI* photometry was taken simultaneously with the spectrograms. The $V-R$ and $R-I$ color indices are very sensitive to the M-type spectral subclass and behave according to the following relations: $V-R=0.0076S^3+1.2$; $R-I=0.16S+0.82$ if $S<$M3; and $R-I=0.36S+0.28$ if $S\geqslant$M3. With this double spectral classification, a spectrum color index scale is obtained. The accuracy of this classification is given. In the later M spectra (M7–M8), the great absorption of TiO bands almost eliminates radiant energy in the visual region. This TiO exists above the stellar photosphere, in the radial structure, mentioned in Paper I (Celis 1982) of this series. Finally, the spectrophotometric characteristics of the singular R Aqr Mira are analyzed in relation to the scale of spectral classification. With this procedure, the classification of 40 Mira stars is given based on the near-infrared photometry.

I. INTRODUCTION

The red variable stars, particularly the Mira-type stars, are commonly of an apparent faint magnitude. Very few are known to be brighter than 6^m0 at the maximum. Among them are *o* Cet, S Car, R Car, R Hor, and R Hya. Previously (Celis 1977), it was observed that, in general, the relatively near Miras ($d<2$ kpc) reach m_V from 7 to 10 mag in phases close to the maximum. The great majority are fainter than 11 mag at maximum. Towards the minima, the spectroscopy becomes more difficult, requiring the use of large telescopes, in order to obtain their spectral properties at these phases, particularly in the Miras of large amplitudes, periods of the order of a year, and with later M spectra. Due to the foregoing, the Miras spectral classification, by using spectrograms, is limited to the phases in which the star is brighter than 10^m0 and in exceptional cases up to 11^m0 (Keenan 1966; Keenan *et al.* 1974).

For the spectral classification of M stars by photoelectric techniques on narrowbands it is also necessary to take bright stars (Jones 1978). Furthermore, the classifications carried out in the M giant stars and Miras reach up to M6 (Deutsch *et al.* 1969; Wing and Yorka 1978; and Rautela and Joshi 1979). The Miras in M7 and M8 are not visually bright, due to their special spectral characteristics (Celis 1980).

On the other hand, the present *UBVRI* wideband photometric system has been recently designed with a high quantum efficiency photocathode (e.g., the 31034A RCA tube) and is very attractive for carrying out observations of faint stars (Bessel 1976; Moffett and Barnes 1979a, b; Kunkel and Rydgren 1979). With these photocathodes, highly sensitive in the red and infrared (see Celis 1982, Paper I), the observations easily reach up to 14 mag in the red stars and with moderately small telescopes (1 m). In paper I it was demonstrated that the $V-R$ and $R-I$ color indices are TiO molecular absorption indices, and the intensity of the molecular absorption indicates the spectral subclass of M stars. It is then possible to carry out a spectral classification based on the photometry of these stars, and this is the main purpose of this work. Previously, Johnson (1966) carried out a calibration between the spectral subtype and the color indices for giant stars, class III in luminosity and relatively near. Nevertheless, no information is given for M7 and M8. The purpose here is to extend this spectrum-photometric classification up to the M8 subclass only for Mira stars. To this end, it was necessary to obtain spectrograms simultaneously with the photometric parameters of these stars at different phases of the luminous cycle. This spectro-photometric combination allows a decimal subclassification which is finer than the one performed by comparison of spectrograms.

II. OBSERVATIONS

The spectroscopic observations were carried out in three periods, during the months of November, December 1981, and January 1982 in the CTIO 1-m telescope. A total of 167 spectrograms corresponding to 28 Mira variable stars were obtained with a grate dispersion image-tube spectrograph. From these, 91 spectrograms were centered in the visual region (86 Å/mm, grating 47, 13°24′ angle, 1st order and centered in 4.500 Å) and 76 in the infrared region (86 Å/mm, grating 47, 1st order with a 19°50′ angle, centered in 7.000 Å). A III a-J emulsion was used in all cases.

An *UBVRI* photometry (see Appendix) in the 0.91-m telescope of the same observatory, was performed with the maximum simultaneity possible with the spectroscopy of the previous paragraph. The photometric study, instrumentation, reductions, and estimated error for these stars were previously given in Paper I.

Although the later M-type standard stars are very scarce, spectrograms from eight of these stars were also obtained. Moreover, the spectrographic profiles, a selection of which is shown later on, were obtained directly from the plates. The Joice Loebl Automatic Recording Microdensitometer (MK 111c) was used, with a Wedge F1070 crystal, 2.52D of the European Southern Observatory, La Silla, Chile. The selected spectrograms were measured with a micrometer belong-

[a] Project supported by the Academic Vice-Presidency, Research Division of the Pontificia Universidad Católica de Chile.
[b] Visiting Astronomer, Cerro Tololo Inter-American Observatory, which is operated by the Association of Universities for Research in Astronomy, Inc., under contract with the National Science Foundation.

 0004-6256/84/040527-22$00.90

ing to the M. Foster Astrophysic Observatory of the Pontifical Catholic University of Chile.

III. PHENOMENOLOGICAL SPECTRAL CLASSIFICATION

Some K and early M standard stars, selected from the catalogue of Seitter (1970, 1975) and Landi *et al.* (1977) were used to identify the earlier subtypes (Table I) mainly to distinguish the K5 types of M0. The phenomenological spectral classification for the Mira stars is essentially based on the presence or intensity of the TiO bands. The criteria of Keenan *et al.* (1974) and Keenan and McNeil (1976) were considered mainly in the blue and visual region. The intensity of the TiO bands in the near infrared was also used as a subclassification guide in the M0–M8 range. Furthermore, the profiles of the spectrograms in the red and infrared were compared with the spectrophotometric Scans obtained by Rautela and Joshi (1979) in the 530–710-nm range. These classification criteria are good within ± 0.5 of the spectral subclass.

The results of this classification are shown in Figs. 1–10. The profiles of the spectrograms selected for the M0 to M8$^+$ classification are shown. The Hα, Hβ, Hγ, and Hδ hydrogen emission lines are indicated in the profiles. The other emission lines present in the near infrared are indicated with their respective wavelengths measured with the micrometer. Moreover, the bandheads of the TiO molecules are indicated. The $V-R$ and $R-I$ color indices observed simultaneously with the spectrograms are given in Table II.

The M0–M8 sequence is ordered according to increasing intensity of the TiO bands. The bands with bandheads $\lambda\lambda$ 4954, 5167, 5448, 5847, 6159, and 7054, which were used for spectral classification are clearly distinguished in almost all figures. In M0 [Figs. 1(a) and 1(b)], the T Gru star shows only the TiO bandheads, which are almost in the form of absorption lines. The continuum of relative flux is similar to the continuum of the HR 1457 standard, of the K5 III type, and equal to HR 1231, M0 III, but having hydrogen emission lines.

Towards the latest of the later spectra in Figs. 1–10, the absorbing bands begin to widen and increase their intensity. In M2 [Fig. 3(a)] the $\lambda\lambda$ 4584 and 4761 bandheads begin to appear; these are very weak in M0 and M1, but clearly defined in M3 with X Cet and M4 with U Cet. In general, as the intensity of the bands increases, it can be observed that the visual continuum relative flux gradually decreases, until it almost disappears in M8 with R Oct.

In spectra which are later than M8, the R Aqr peculiar variable shows in the visual region only emission lines [Fig. 10(a)]. The λ 5448 can hardly be observed and the visual continuum relative flux cannot be observed as clearly as in stars of earlier types. On the other hand, starting from M5.5, absorption bands without bandheads begin to appear with maximum depressions at λ 5625 and λ 7438. The intensity of these bands increases greatly for later subtypes. In M7, the λ 7978 band also appears. Finally, the band without bandhead in λ 6713 is observed with increasing intensity throughout the whole sequence from M0 to M8. The emission lines show the opposite behavior, they decrease in intensity from M0 to M6, until they disappear in M7. Nevertheless, emission lines in Miras generally become weak or disappear following minimum light. Therefore, this weakening could well be due to observations of the late-type spectra at phases near minimum light, rather than due to some intrinsic connection between emission line strength and spectral class. Sometimes Hα appears weakly in M7 for normal Miras [Fig. 8(b)]. In addition, in M8, it is also possible to find weak emissions at $\lambda\lambda$ 4571, 7332, 7343, and 7371 [R Hor, Fig. 9(b)] which do not exist in earlier spectra. The last three of these emissions in R Hor are clearly visible in the R Aqr peculiar variable [Fig. 10(b)].

IV. PHOTOMETRIC SPECTRAL CLASSIFICATION

In Paper I, it was shown that the $(V-R)$ and $(R-I)$ color indices are very sensitive to the M-type spectral subclass. These indices give the intensity of the absorbing bands, mainly of TiO, rather than the color temperature. The two-color $(V-R, R-I)$ diagram shows a sequence clearly defined for all subclasses of Me stars. On the other hand, the two-color $(U-B, B-V)$ diagram does not show such an explicit relationship as those found for near infrared (Celis 1975). The most sensitive color index corresponds to $V-R$ having a range of 4 mag from M0 to M8. Therefore, the spectral subclass derivation according to these indices depends on the scale adopted in the range considered.

In order to construct such a scale, with all the spectrograms obtained, a selection of the most representative ones of each subtype was done. In Table III column 6 is shown the number of spectrograms chosen for each subtype. During the observations, only one star was found in the M0 and M1 subclass, respectively, due to the fact that only 6% of the red variables reach subclasses smaller than M3 at maximum (Celis 1980). Furthermore, Table III provides the average colors of $V-R$ and $R-I$ and its variation range for $S \geqslant$ M2.

Figures 12 and 13 show the correlation between the average color indices of Table III with the spectral subtype. In addition, the individual values of Table II corresponding to each one of Figs. 1–9 are represented. This result is compared with Johnson's (1966) determination for red giant stars (luminosity class III) in the M0–M6 range. Continuous curves are drawn according to the following equations:

$$V-R = 0.0076S^3 + 1.2, \tag{1}$$

and

$$R-I = \begin{cases} 0.16S + 0.82 & \text{if } S < \text{M3} \\ 0.36S + 0.28 & \text{if } S \geqslant \text{M3}, \end{cases} \tag{2}$$

respectively. Although these equations do not allow clear distinguishing of M0 from M1, they give an account of almost 100% of subclass in Mira variables, especially in phases far away from the maximum. Moreover, they allow decimal values of the spectral subclassification to be obtained. Table VI shows the spectral classification of Mira variables using the $V-R$ and $R-I$ indices, for every quarter of a subclass. Table IV gives the spectral classification based on color in-

TABLE I. Spectroscopical standards.

Star HR	V	$B-V$	$V-R$	$R-I$	Sp	Notes
2037	4.78	—	—	—	K3 II	1
1457	0.86	1.54	1.23	0.94	K5 III	1
1231	2.94	1.60	1.26	1.00	M0 III	2
911	2.53	1.64	1.35	1.16	M1.5 III	2
1247	4.55	1.52	—	—	M2 III	2
519	5.49	1.54	1.49	1.27	M3 III	2
8636	2.11	1.62	1.91	1.77	M5 III	2
8481	5.09	1.64	4.44	2.81	M6 III	2

1. Seitter (1970).
2. Landi *et al.* (1977).

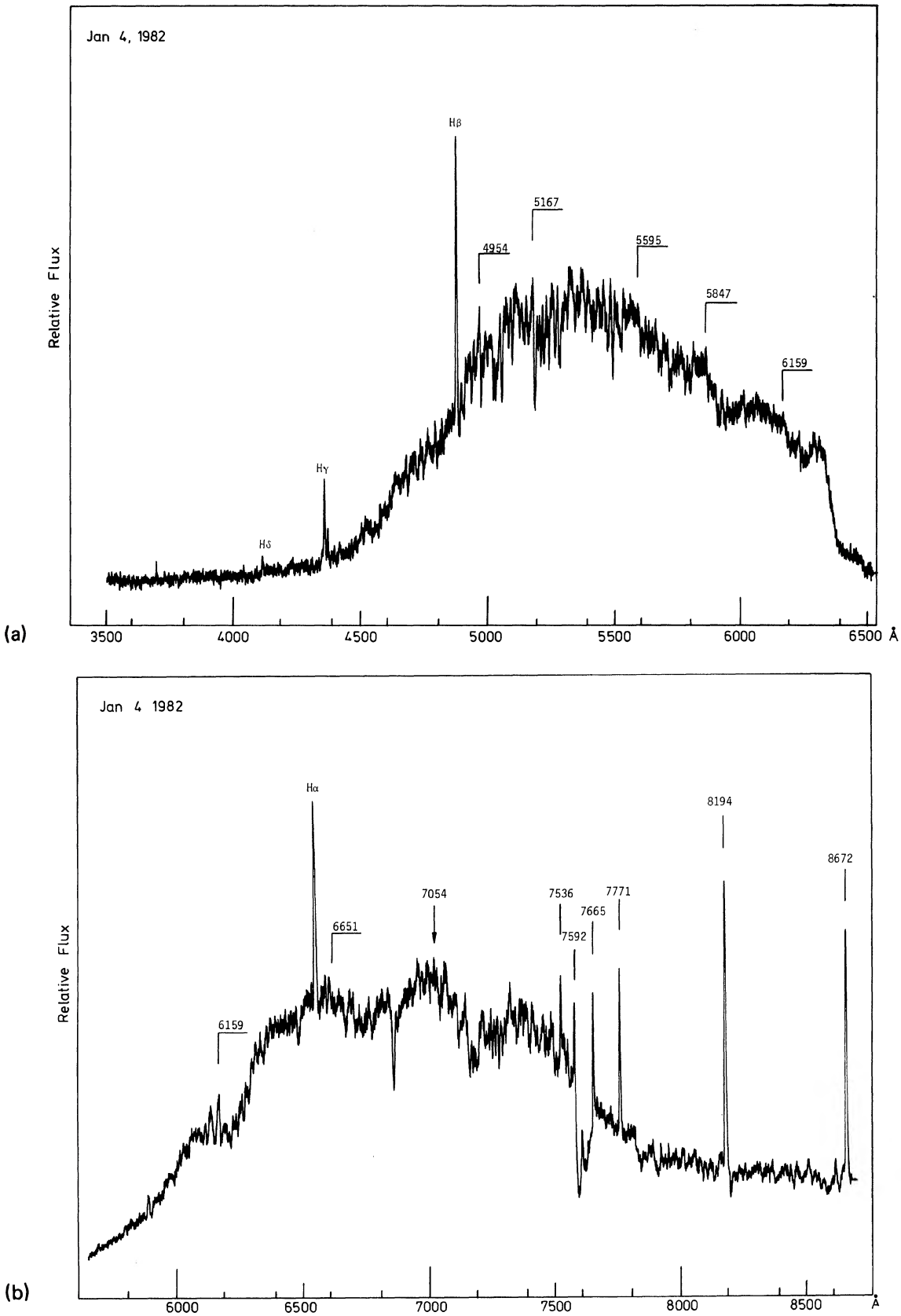

FIG. 1. T Gru, M0e; (a), visual region, (b), infrared region.

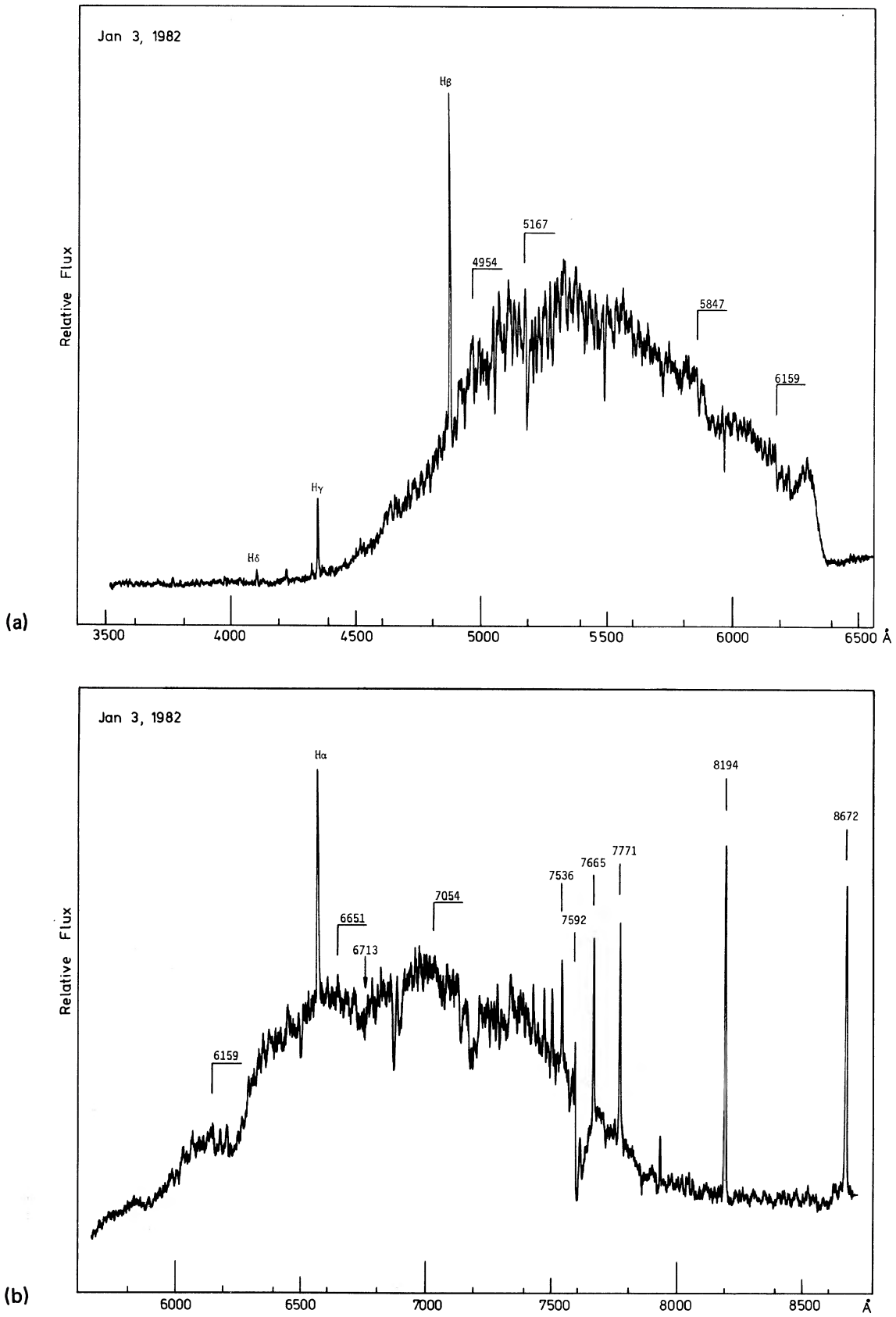

FIG. 2. S Car, M1e; (a), visual region, (b), infrared region.

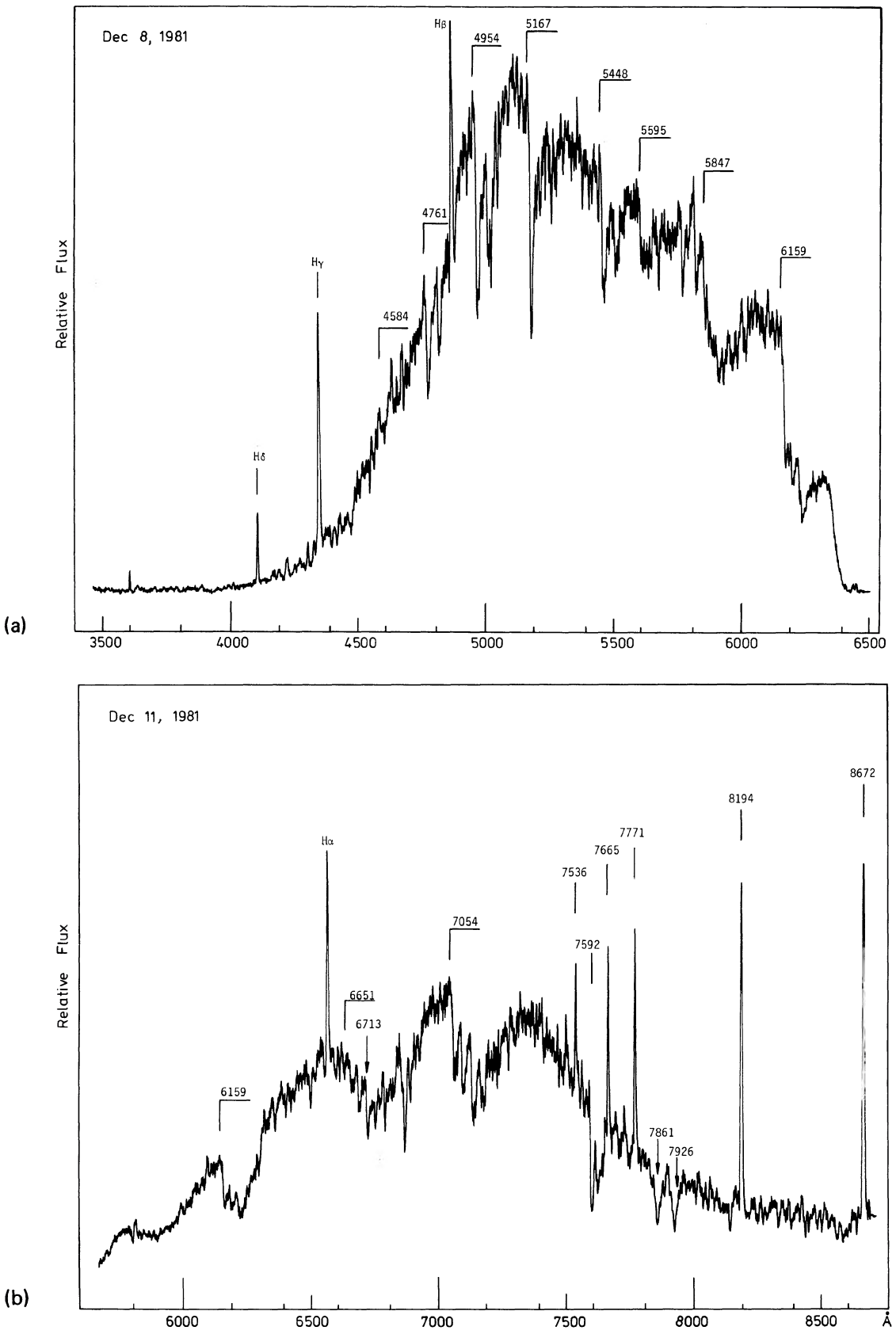

FIG. 3. S Car, M2e; (a), visual region, (b), infrared region.

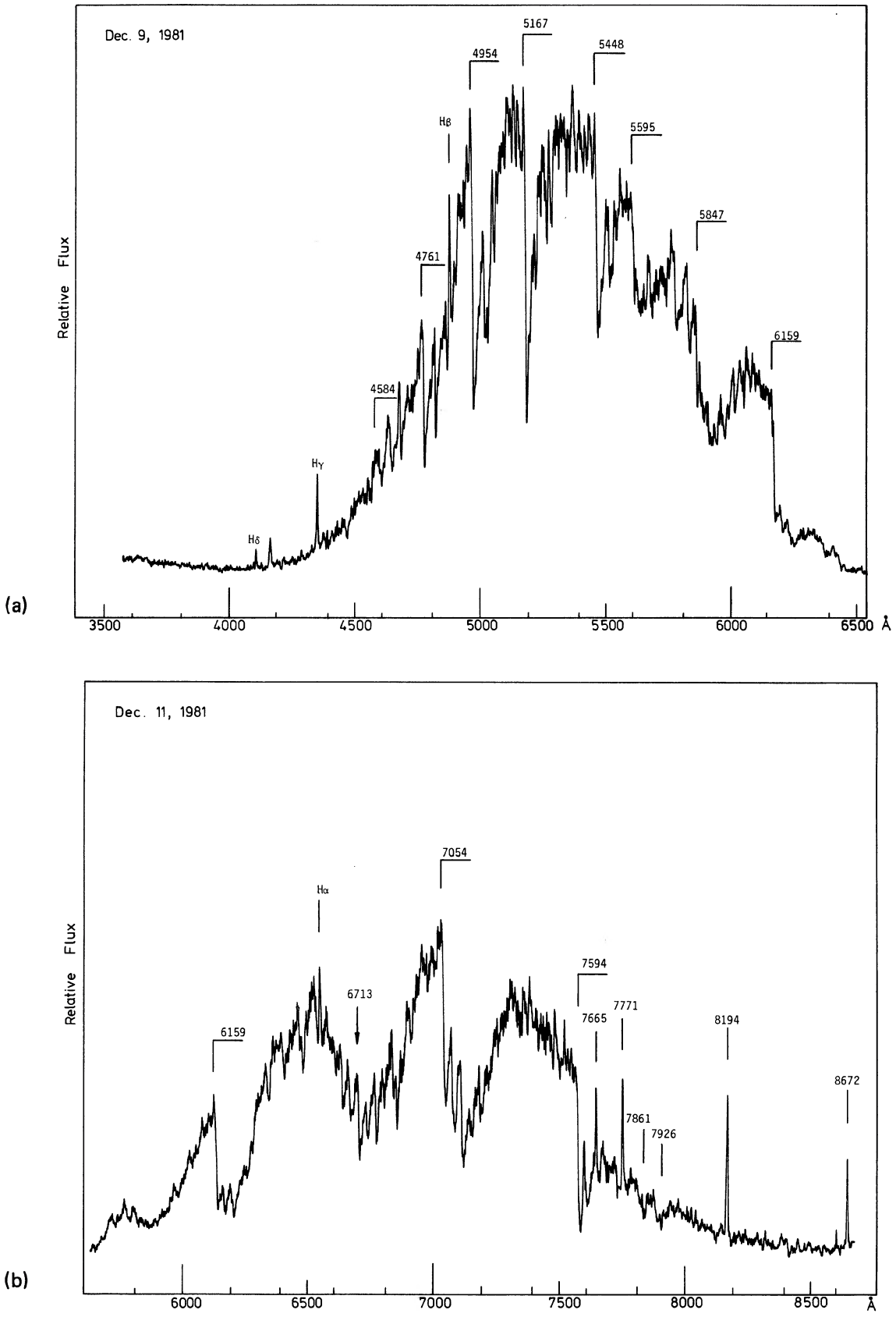

FIG. 4. X Cet, M3e; (a), visual region, (b), infrared region.

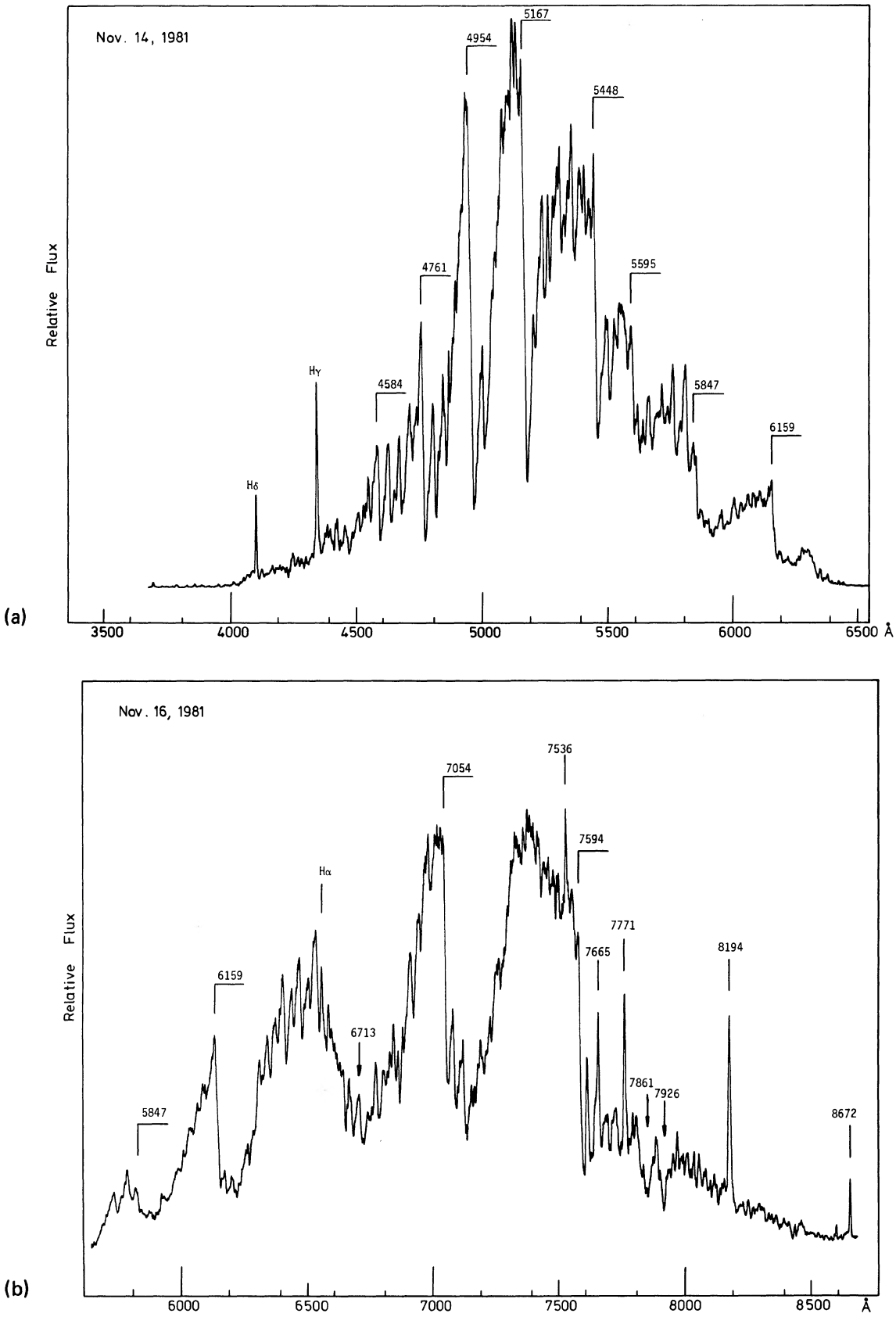

FIG. 5. U Cet, M4e; (a), visual region, (b), infrared region.

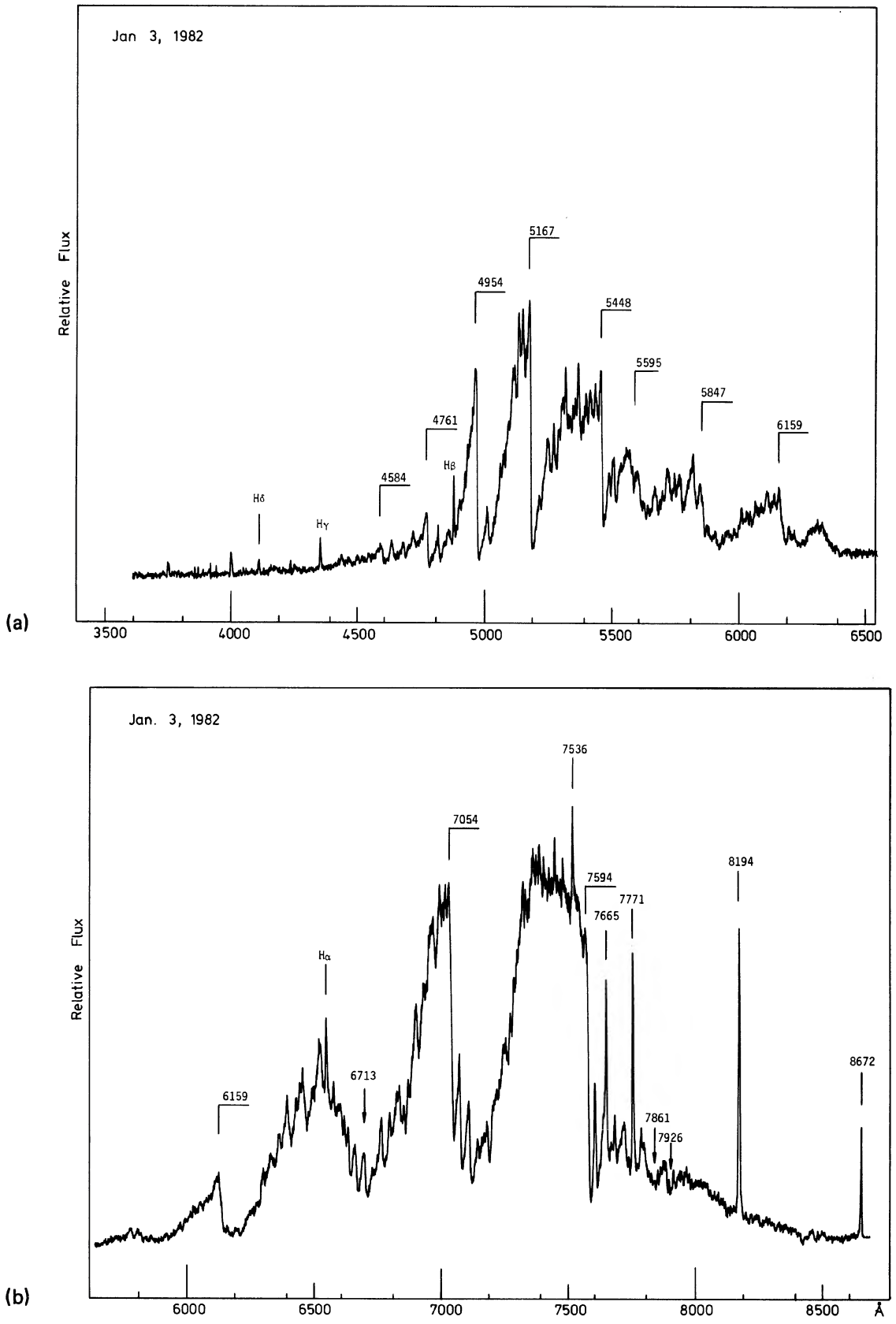

FIG. 6. T Hya, M5e; (a), visual region, (b), infrared region.

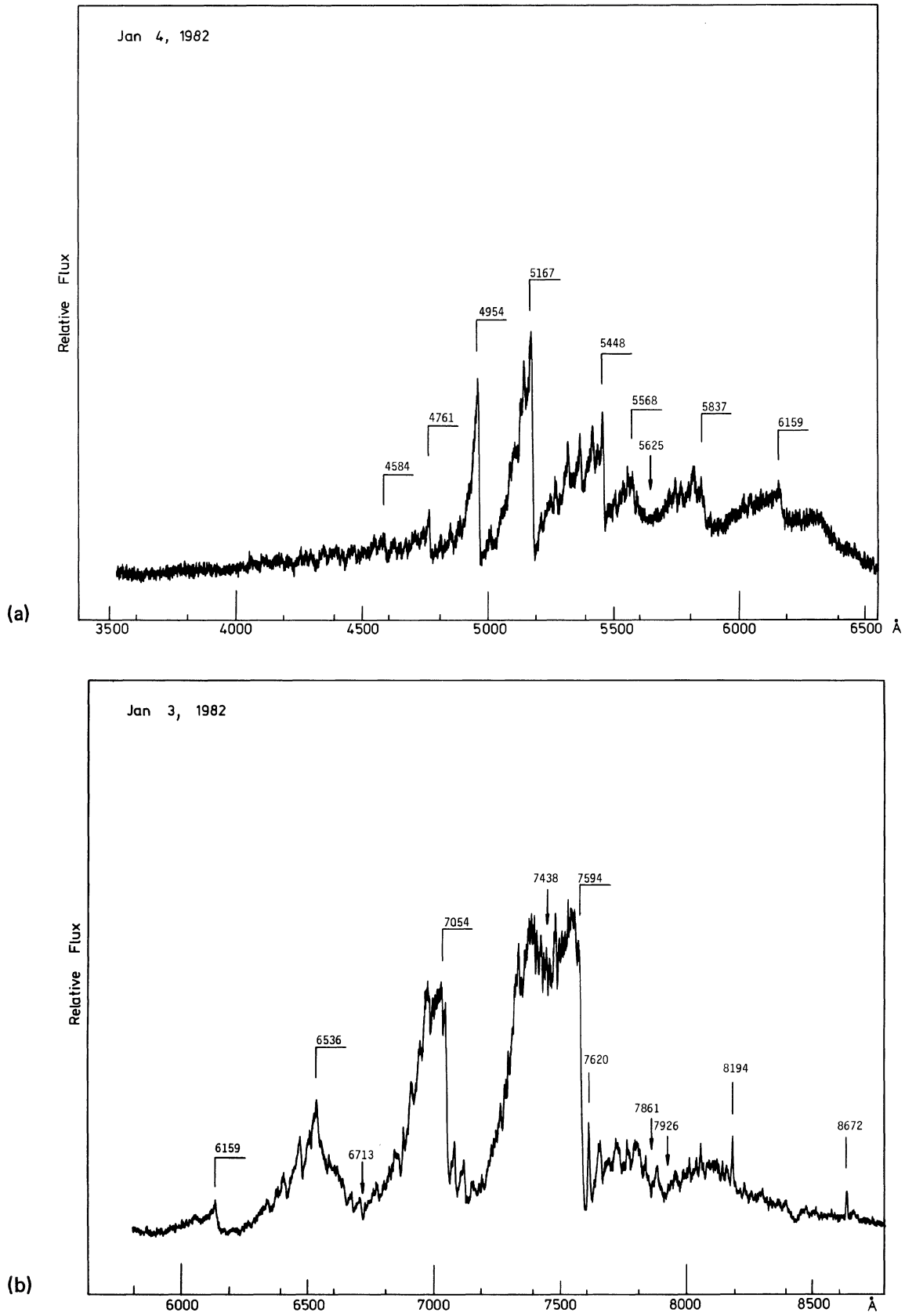

FIG. 7. T Scl, M6e; (a), visual region, (b), infrared region.

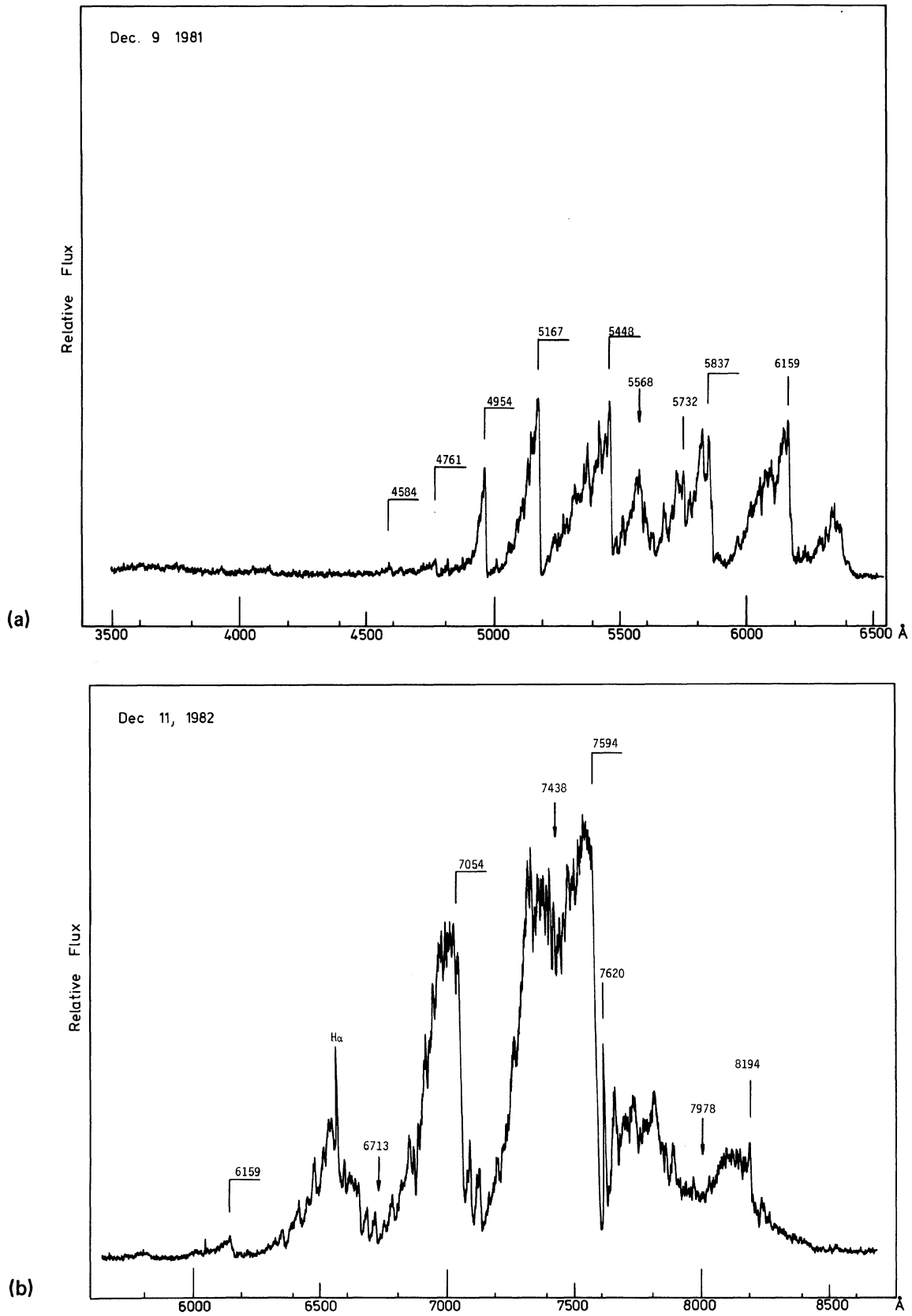

FIG. 8. R Oct, M7e; (a), visual region, (b), infrared region.

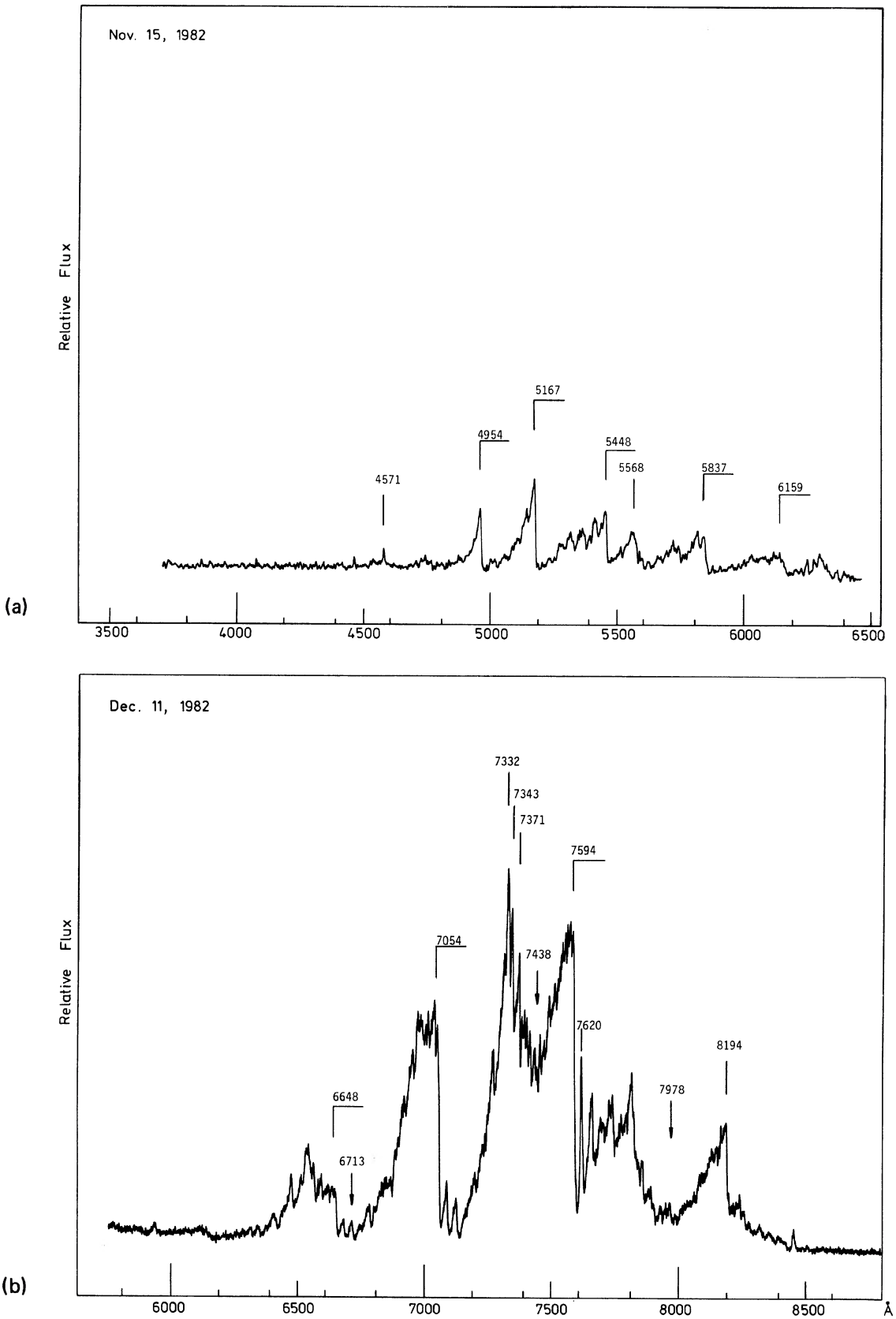

FIG. 9. R Hor, M8e; (a), visual region, (b), infrared region.

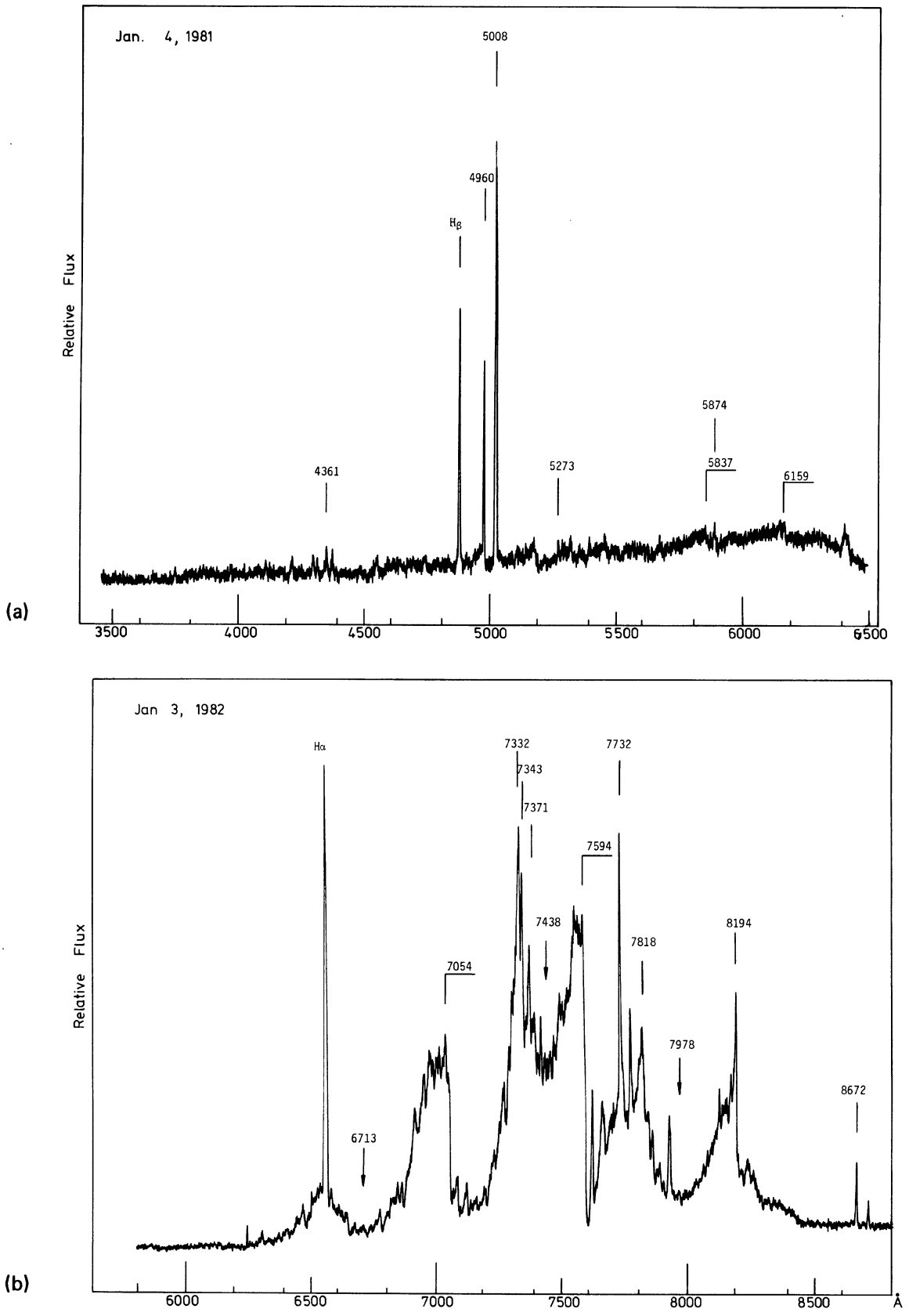

FIG. 10. R Aqr, M8e$^+$; (a) visual region, (b), infrared region.

TABLE II. $V-R$ and $R-I$ colors as functions of M spectral subtype of the variable stars shown in Figs. 1–9.

S	Star	Fig.	$V-R$	$R-I$
M0	T Gru	1	1.07	0.83
M1	S Car	2	1.15	0.91
M2	S Car	3	1.25	1.11
M3	X Cet	4	1.52	1.37
M4	U Cet	5	1.65	1.85
M5	T Hya	6	2.12	2.00
M6	T Scl	7	2.75	3.33
M7	R Oct	8	3.84	2.75
M8	R Hor	9	5.19	3.21

TABLE III. Mean values and range of $V-R$ and $R-I$ as functions of the spectrum.

S	$(V-R)$	$V-R$ range	$(R-I)$	$R-I$ range	n
M0	1.07	1.00–1.10[a]	0.83	0.74–0.83[a]	1
M1	1.15	1.11–1.22[a]	0.91	0.83–0.99[a]	1
M2	1.26	1.23–1.31	1.15	0.84–1.22	3
M3	1.45	1.41–1.52	1.41	1.37–1.49	3
M4	1.72	1.64–1.82	1.77	1.66–1.85	5
M5	2.12	1.97–2.27	2.00	1.97–2.02	3
M6	2.80	2.75–2.86	2.40	2.33–2.46	4
M7	3.79	3.63–3.97	2.77	2.78–2.80	6
M8	5.05	9.93–5.19	3.11	3.07–3.22	4

[a] Range obtained from extrapolating the $(V-R, R-I)$ diagram shown in Paper I.

dices of near infrared of 40 Mira variables and the spectral types derived from the plates for 28 stars. Equations (1) and (2) were used to obtain the $S(V-R)$ and $S(R-I)$ for all observations. Table IV is plotted in Fig. 14, where these spectra can be compared. The 45° line is traced. This figure shows that

(a) $S(V-R)=S(R-I)$ with good accuracy; then one can take as the final spectral subclass for any phase of light cycle the following:

$$S=\tfrac{1}{2}\,[S(V-R)+S(R-I)].$$

(b) The most important subclass of Mira variables begins at M3. From the 46 observed Mira variables, only T Gru ($P=136.6\,d$), R Pic ($P=164.2\,d$), and S Car ($P=149.6\,d$) show subclass earlier than M3 at maximum. However, there might be a mean difference of up to 0.2 subclass, according to the color index chosen. This mean difference depends on the precision of the subclassification taken into account.

The $\sigma(V-R)$ and $\sigma(R-I)$ standard deviations of all variable stars found in each subclassification of Table III were used to estimate the accuracy of the spectral subclass extracted from the color indices. An adequate number of stars was found only starting from M2 on, in order to calculate the standard deviation in each subtype. The product of the derivative of expressions (1) and (2) with respect to the color indices and the $\sigma(V-R)$ and $\sigma(R-I)$ standard deviations, propagates the dispersion to the spectral subtype. In other words,

$$\sigma(S)_{V-R}=\frac{dS}{d(V-R)}\sigma(V-R), \tag{3}$$

and

$$\sigma(S)_{R-I}=\frac{dS}{d(R-I)}\sigma(R-I). \tag{4}$$

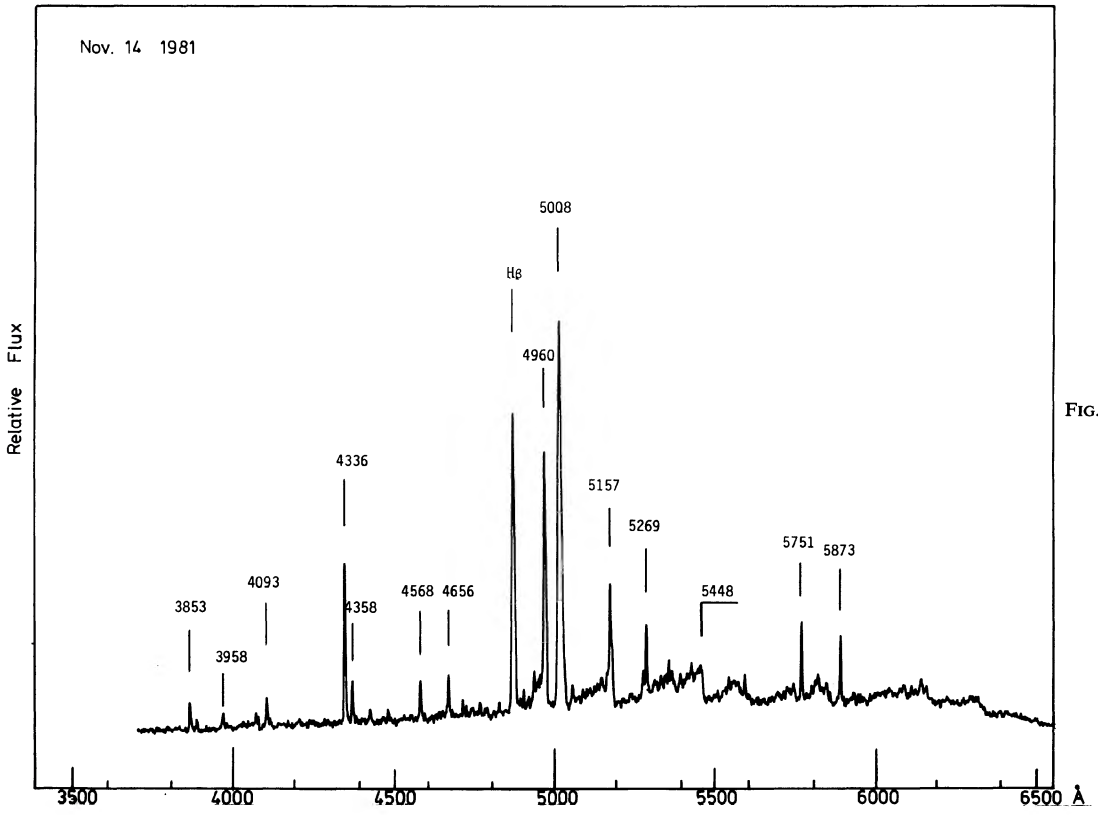

FIG. 11. R Aqr, M8e$^+$.

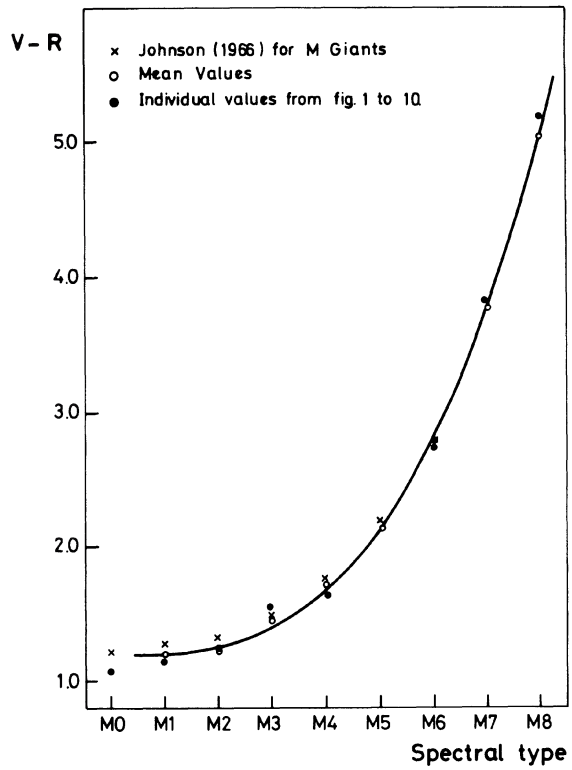

FIG. 12. Spectral type, $V-R$ relation; the curve is $V-R = 0.0076S^3 + 1.2$.

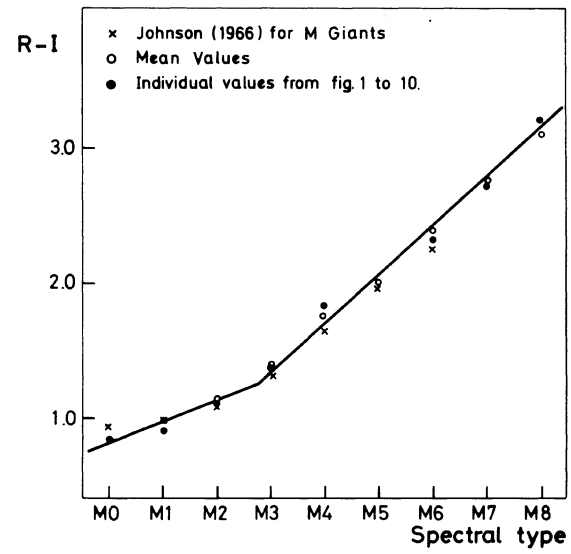

FIG. 13. Spectral type, $R-I$ relation; the curves are $R-I = 0.16S + 0.82$ if $S <$ M3 and $R-I = 0.36S + 0.28$ if $S \geq$ M3.

The $\sigma(S)$ deviation, inferred from expressions (3) and (4) is $\sigma(S) = (\sigma(S)^2_{V-R} + \sigma(S)^2_{R-I})^{1/2}$. The result of this whole procedure is shown in Table V for M2 up to M8. In M0 and M1, the accuracy is probably similar to that of M2, according to the tendency shown in the two-color ($V-R$, $R-I$) diagram.

V. THE R AQR SYMBIOTIC SYSTEM

Figures 10 and 11, added to the M0–M8 sequence, show the profiles of spectrograms taken from R Aqr. These spectrograms are mainly characterized by the presence of a considerable number of emission lines existing through the whole spectrum. The identification of S II, He I, Na I, N II, O I, O III, Fe II, Fe III, Mg I, C II, Ca I emission lines and hydrogen lines was obtained by Wallerstein and Greenstein (1980), in the range between 3736 and 6727 Å. Until now, it is not known if this is due to the fact that R Aqr is a binary Mira or a simple star with an active magnetic region (Zuckerman 1980; Wallerstein and Greenstein 1980). The situation of the possible hot star companion of R Aqr is still undefined (Johnson 1981). Furthermore, radio and optical observations indicate the existence of a jet-like feature extending 10″ from the central star (Sopka *et al.* 1982). Previously, Merrill (1940) demonstrated that the central star is surrounded by a hot gas, a disseminated nebula, and an elliptical ring.

Figures 10 and 11 also show that the relative continuum hardly exists in the visual region due to the great intensity of the TiO bands. This mere fact would allow us to classify R Aqr with a subtype later than M8 if compared with R Hor (Fig. 9). However, the emission lines of the visual region lower the $V-R$ color index as low as $4^m.74$, a fact which, according to the scale of Table VI would result in an M8$^-$ subtype.

On the other hand, one must take into account that in later M-type normal Miras the following holds: (a) They are covered by several layers of TiO (Paper I). (b) The great absorption of the absorbing layers makes the visual magnitude become high (Celis 1980). (c) The visual amplitude strongly depends on the amplitude excess (Celis 1978–1979) producing extremely faint minima. (d) The M_V absolute visual magnitude is greatly influenced by the effect of TiO ($\delta_{TiO} M_V$) (Smak 1964; Smak and Wing 1979).

From all this, it can be inferred that they are faint in luminosity, not necessarily because they might be too far away, but alternatively, because the radiant energy in the visual region is not allowed to emerge and produces an absence of continuum in this region.

Thus, it is the energetic contribution of the R Aqr emission lines, which gives a greater luminosity to the star. Consequently, the $V-R$ color index is relatively low, and the $U-B$ index has negative values (up to $-0^m.6$; see Paper I). Therefore, the R Aqr spectral type cannot be earlier than M8$^+$.

VI. PHOTOMETRIC CALIBRATIONS OF Me SPECTRAL SUBCLASSES

Table VI compares the present photometric calibration of Me spectral subclass in columns 2 and 3 with the calibrations made by Johnson (1966) (columns 4 and 5) and Barnes (1973) for Mira Variables. This comparison is shown in Fig. 15. Johsnon's color indices are based on 225 stars of luminosity class III with spectral types ranging from G5 to M6. All the subclassification of Johnson was made according to *increasing values* of color indices. Johnson reaches to $(V-R) = 2.8$ for M6. But Miras reach to $(V-R) = 5.2$ at the minimum. These stars are very red, but not necessarily faint because of their distance. The nearest Mira are o Cet ($m_0 - M = 4.4$)

TABLE IV. Spectral classification of Me Mira variables with the color indices $V-R$ and $R-I$ and the spectrograms taken in 1981–1982. The observation with asterisk (*) was included in the calibration of the photometry.

STAR	DATE	V	S(V-R)	S(R-I)	PLATE-CAMP V: Visual I: Infrared	S	NOTE
R Aqr	Oct.11/12	11.69	M6.4	M6.1			
	13/14	11.78	M7.5	M7.6	4271-2I	M8e	
		11.61	M7.6	M7.7			
	14/15	11.56	M7.5	M7.7			
	Nov.12/13	11.95	M7.7	M8.1			
	13/14				4400-5V	M8e	
	14/15				4404A-2V	M8e	
	Dec. 7/8	11.88	M7.7	M8.1			
	7/8	11.89	M7.7	M8.1	4493-4V	M8e	
	8/9				4497-4V	M8e	
	10/11				4503-4I	M8+e	
	Jan. 2/3				4508-6I	M8+e	
	3/4	11.48	M7.7	--	4714-6V	M8+e	
	3/4	11.54	M7.8	M8.0			
T Aqr	Oct.10/11	11.53	M6.1	M6.0			
	13/14	11.51	M6.0	M6.0			
	Nov.15/16				4408-2V	M6:	
Z Cap	Oct.10/11	10.13	M3.5	M3.6			
	11/12	10.22	M3.6	M3.5			
	13/14				4270-6I	M3.5e	
	Nov.12/13	9.23	M2.9	M2.5			
	13/14				4400-4V	M3-e	
	15/16	9.27	M2.9	M2.6	4408-4I	M3-e	
	15/16	9.28	M3.2	M2.6			
	Dec. 7/8	9.76	M3.9	M3.4			
	9/10				4501-2V	M4e	
	10/11				4502-4I	M4e	
S Car	Nov.12/13	7.27	M4.2	M4.4	4399-5V	M4+e	
	12/13	7.25	M4.2	M4.3			
	14/15	7.18	M4.1	M4.3			
	14/15	7.17	M4.1	M4.2			
	15/16				4411-5I	M4+e	
	Dec. 7/8	5.88	M1.9	M1.8	4495-6V	M2e	*
	10/11				4507-2I	M2e	*
	Jan. 2/3	5.93	M2.4	M1.7	4712-2I	M1e	*
					4712-6V	M1e	*
RS Cen	Nov.12/13	8.10	M3.4	--			
	13/14	8.12	M3.4	M3.1			
	14/15	8.16	M3.5	M3.2			
	15/16				4411-6I	M3+e	
	Dec. 7/8	8.61	M4.0	M4.0	4495-7V	M4e	
	8/9				4497-7V	M4e	
	10/11				4507-4I	M4:	
	Jan. 2/3	10.01	M5.2	M4.7	4712-4I	M5e	*
	2/3				4712-5V	M5e	*
S Cet	Oct. 9/10	9.78	M5.6	--			
	13/14	8.97	M5.1	M4.8			
	Nov.13/14	10.74	M6.1	M6.0			
	Dec.10/11	12.19	M6.6	M6.6			
	Jan. 2/3	13.25	M7.1	M6.8			
R Cet	Oct.13/14	8.02	M3.7	M4.1			
	Nov.13/14				4400-7V	M4e	*
	15/16	8.03	M3.7	M4.2	4409-4I	M4e	*
	Dec. 7/8				4493-7V	M4+e	
	9/10	8.20	M4.4	M4.3	4497-6V	M4+e	
	10/11	8.19	M4.4	M4.4	4503-7I	M4.5e	
	Jan. 2/3				4509-4I	M5:	
	3/4	10.13	M6.0	M5.9	4715-2V	M6:	
	3/4	10.14	M6.0	M5.9	4715-2V	M6:	
U Cet	Oct.10/11	10.74	M5.9	M6.1			
	10/11	10.69	M5.9	M6.1			
	12/13				4268-5I	M6:	
	Nov.13/14	8.28	M3.9	M4.4	4401-2V	M4 e	*
	15/16				4409-5I	M4e	*
	Dec. 8/9				4497-7V	M3e	*
	10/11	7.17	M3.1	M3.4	4504-2I	M3e	*
	Jan. 2/3				4509-5I	M4:	
	3/4	7.57	M3.9	M3.9	4715-5V	M4-e	
	3/4	7.55	M3.9	M3.9	4715-6V	M4e	

TABLE IV. (continued)

STAR	DATE	V	S(V-R)	S(R-I)	PLATE-CAMP V: Visual I: Infrared	S	NOTE
V Cet	Nov.15/16	14.76	M7.3	M7.5			
	15/16	15.05	M7.6	M7.6			
	Jan. 2/3	13.40	M7.1	M6.9			
X Cet	Oct.10/11	11.28	M5.4	M5.4			
	11/12	11.15	M5.4	M5.3			
	13/14				4271-5I	M5^{+}e	
	Nov.12/13	9.54	M3.7	M3.9			
	12/13	9.56	M4.0	M4.0			
	13/14				4402-5V	M4e	*
	15/16	9.43	M3.6	M3.8	4409-7I	M4e	*
	Dec. 8/9				4498-5V	M3e	*
	10/11	9.01	M3.5	M3.4	4504-6I	M3e	*
	10/11	9.03	M3.4	M3.6			
	Jan. 2/3				4510-6I	M3.5:	
	3/4	8.96	M3.8	M3.6	4716-5V	M4^{-}e	
	3/4				4716-6V	M4^{-}e	
Z Cet	Oct.10/11	10.85	M5.9	M5.8			
	10/11	10.88	M6.0	M5.8			
	Nov.13/14	12.98	M7.0	M6.9			
	Dec.10/11	13.75	M7.1	M7.3			
	Jan. 2/3	12.84	M7.0	M6.9			
o Cet	Oct.10/11	4.69	M6.0	--			
	11/12				4265-7I	M6	
	12/13				4268-4I	M6:	
	13/14	4.75	M6.0	--			
	14/15	4.85	M6.1	--			
	Nov.12/13	5.90	M6.8	--	4397-7V	M6.5e	
	14/15				4409-2I	M7e	
	Jan. 2/3				4508-2I	M7:	
	3/4	7.69	M7.3	M7.2	4714-2V	M7^{+}	
	3/4				4714-4V	M7^{+}	
R Cha	Nov.13/14	13.37	M7.9	M7.8			
	Dec. 7/8	12.88	M7.6	M7.7			
	Jan. 2/3	10.55	M6.3	M6.3			
T Col	Oct.10/11	7.42	M4.2	M4.0			
	11/12	7.72	M4.2	M4.3	4266-5I	M4e	
	Nov.12/13	7.82	M4.7	M4.8	4398-5V	M5	*
	15/16	7.92	M4.7	M4.9	4410-6I	M5e	*
	Dec. 7/8	8.33	M5.3	M5.4	4494-5V	M5^{+}	
	8/9				4506-2I	M5.5	
	Jan. 2/3	9.48	M6.0	M6.1	4511-4I	M6	*
	3/4				4718-5V	M6	*
	3/4				4718-6V	M6	*
T Eri	Oct.10/11	8.11	M4.2	M4.4			
	11/12	8.28	M4.1	M4.3			
	12/13				4269-2I	M4e	
	13/14	8.20	M4.0	M4.2			
	14/15	8.21	M4.0	M4.1			
	Nov.13/14				4402-6V	M5	
	14/15	8.17	M4.5	M4.7			
	15/16				4409-8I	M5.5	
	Dec. 8/9				4498-6V	M6	*
	10/11	9.67	M5.9	M5.9	4504-7I	M6	*
	10/11	9.66	M5.8	M5.9			
	Jan. 2/3				4510-4I	M6.5	
	3/4	10.88	M6.6	M6.3	4716-7V	M6.5	
	3/4	10.87	M6.4	M6.3	4716-8V	M6.5	
T Gru	Oct. 9/10	11.37	M4.8	M4.7			
	10/11	11.44	M4.8	M4.7			
	11/12	11.51	M4.8	M4.7			
	12/13				4267-7I	M5^{-}e	
	Nov.12/13	10.18	M3.4	M3.4			
	14/15				4404A-4V	M3e	*
	15/16	9.88	M3.0	M3.9	4408-7I	M3e	*
	Dec. 7/8	9.18	M1.6	M1.8	4493-2V	M2e	*
	10/11				4502-5I	M2e	*
	Jan. 2/3	8.47	M0.0	M0.0	4508-4I	M0e	*
	3/4				4714-5V	M0e	*
R Gru	Oct. 9/10	13.09	M7.4	M7.4			
	14/15	13.05	M7.4	M7.4			
	Nov.13/14	11.59	M7.1	M7.4			

TABLE IV. (continued)

STAR	DATE	V	S(V-R)	S(R-I)	PLATE-CAMP V: Visual I: Infrared	S	NOTE
S Gru	Oct. 9/10	13.57	M8.1	M8.4			
	12/13	13.51	M8.1	M8.4			
	Nov.14/15	12.09	M8.1	M8.3			
R Hor	Oct.12/13	12.30	M7.9	M7.9	4268-6I	M8	
	12/13	12.25	M8.0	M8.0			
	14/15	12.35	M8.0	M7.9			
	Nov.13/14				4402-2V	M8	*
	14/15	12.20	M8.0	M7.8	4404A-6V	M8	*
	14/15				4405-2V	M8	*
	Dec. 7/8	11.77	M8.1	--			
	7/8	11.76	M8.0	M8.1			
	8/9				4498-2V	M8+	
	10/11				4504-4I	M8+	
	Jan. 2/3	10.96	M7.9	--	4509-6I	M8	*
	2/3	10.96	M7.9	M7.8			
	3/4				4715-7V	M8	*
	3/4				4715-8V	M8	*
T Hor	Oct.10/11	12.22	M6.4	M6.2			
	12/13	12.13	M6.4	M6.2	4268-7I	M6+	
	Nov.13/14	10.25	M5.6	M5.6	4402-4V	M5.5	
	15/16	10.14	M5.5	M5.5			
	Dec. 8/9				4498-4V	M4	*
	10/11	9.20	M4.3	M4.4	4504-5I	M4	*
	10/11	9.17	M4.3	M4.3			
	Jan. 2/3	8.69	M3.8	M3.8	4509-7I	M4-e	
	3/4				4716-2V	M3.5e	
	3/4				4716-4V	M3.5e	
S Hya	Nov.14/15	11.85	M6.7	M6.6			
T Hya	Nov.12/13	7.69	M3.8	M3.9	4399-4V	M4-e	
	15/16				4411-4I	M4e	
	Dec. 7/8	7.52	M4.1	M3.8	4495-5V	M4e	*
	10/11				4506-7I	M4e	*
	Jan. 2/3	8.32	M4.9	M4.8	4511-8I	M5e	*
	2/3				4712-7V	M5e	*
X Hya	Nov.13/14	8.60	M6.0	M5.8			
	Dec.10/11	8.53	M6.1	M6.1			
	Jan. 2/3	9.25	M6.6	M6.4			
R Ind	Oct.10/11	10.12	M4.7	M4.7			
	12/13	10.39	M4.9	M4.8			
	14/15	10.48	M4.9	M4.8			
	Nov.13/14	12.09	M6.3	M6.3			
	14/15				4404A-5V	M6	
	15/16	12.20	M6.3	M6.3			
	Dec. 8/9	13.25	M6.7	M6.7			
	9/10				4501-4V	M6.5	
	10/11				4503-2I	M6.5	
	Jan. 2/3				4508-5I	M6+	
	3/4	13.24	M6.7	M6.4			
R Leo	Nov.12/13	8.19	M7.3	--			
	Jan. 2/3	9.33	M7.6	M7.5			
	2/3	9.36	M7.6	M7.6			
	3/4				4719-2V	M7.5	
T Lep	Oct.12/13	9.62	M6.6	M6.3			
	13/14				4272-5I	M6.+	
	14/15	9.72	M6.7	M6.3			
	Nov.13/14	9.86	M6.7	M6.5	4403-4V	M6.5	
	14/15	9.97	M6.8	M6.4	4405-4V	M6.5	
	15/16				4410-5I	M6.5	
	Dec. 7/8	10.41	M7.0	--	4494-4V	M7	*
	7/8	10.45	M7.0	M7.0			
	8/9				4499-6V	M7:	
	10/11				4505-7I	M7	*
	Jan. 2/3	10.90	M7.0	M7.1	4511-2I	M7	*
	3/4				4718-2V	M7	*
	3/4				4718-4V	M7	*
R Mic	Oct.10/11	12.29	M6.3	M6.0			
	13/14	12.65	M6.4	M6.1	4270-5I	M6:	
	14/15	12.70	M6.4	M6.2			

TABLE IV. (continued)

STAR	DATE	V	S(V-R)	S(R-I)	PLATE-CAMP V: Visual I: Infrared	S	NOTE
	Nov.13/14	13.22	M6.9	M6.8	4400-2V	M7	*
	13/14	13.17	M6.8	M6.8			
	15/16	13.04	M6.7	M6.8			
	Dec. 7/8	11.28	M5.6	M6.0			
	8/9				4497-2V	M6	*
	10/11				4502-2I	M6	*
V Mon	Oct.10/11	11.38	M7.3	M7.1			
	11/12	11.35	M7.3	M7.1	4266-7I	M7	
	Nov.12/13	9.61	M6.4	M6.3	4398-7V	$M6^+$	
	15/16				4410-7I	M6	
	Dec. 7/8	7.70	M5.3	M5.4	4494-7V	$M5^+$	
	10/11				4506-5I	M5	
	Jan. 2/3	6.87	M4.7	M4.8	4511-6I	$M5^-$	
	2/3				4713-2V	M4.5	
	3/4				4718-8V	M4.5	
R Oct	Oct.11/12	9.45	M6.5	M6.3	4266-6I	M6:	
	Nov.13/14	10.07	M6.7	M6.4	4403-5V	$M6^+$	
	14/15	10.06	M6.7	M6.4	4404B-5V	$M6^+$:	
	14/15				4405-5V	$M6^+$:	
	Dec. 7/8	10.75	M7.0	M6.9	4494-6V	M7	*
	7/8	10.76	M7.0	M6.9			
	8/9				4499-7V	M7:	*
	8/9				4500-2V	M7	*
	10/11				4506-4I	M7:	*
	Jan. 2/3	11.34	M7.1	M7.0	4511-5I	M7	*
	2/3				4713-4V	M7	*
	3/4				4718-7V	M7	*
S Oct	Oct. 9/10	8.06	M4.4	M3.9			
	12/13	8.19	M4.5	M4.0			
	14/15	7.93	M4.5	--			
S Ori	Oct.12/13	11.21	M6.3	M6.3			
	14/15	11.01	M7.2	M7.0			
	Nov.14/15	11.45	M7.2	M7.1			
	Dec.10/11	11.91	M7.6	M7.7			
	10/11	11.94	M7.6	M7.7			
	Jan. 3/4	12.08	M7.7	M7.6			
R Pav	Oct. 9/10	12.40	M6.8	M6.6			
	12/13	12.58	M6.8	M6.6			
	Nov.12/13	12.75	M7.2	M6.9			
W Pup	Oct.11/12	11.88	M6.1	M6.0			
	13/14				4272-6I	M6:	
	Nov.12/13	9.78	M4.6	M4.5	4399-2V	M4.5e	
	12/13	9.78	M4.8	M4.7			
	15/16	9.39	M4.5	M4.5	4410-8I	M4.5e	
	Dec. 7/8				4495-2V	M2e	*
	7/8	7.73	M2.4	M2.6	4495-4V	M2e	*
	10/11				4506-6I	M2e	*
	Jan. 2/3	8.12	M3.8	M3.3	4511-7I	$M3^+e$	
	2/3				4712-8V	$M3^+e$	
R Ret	Oct.11/12	13.27	M7.4	M7.4			
	12/13	13.61	M7.4	M7.5	4269-4I	$M7^+$	
	Nov.12/13	13.13	M7.8	M7.5			
	13/14				4403-2V	M7.5	
	14/15	12.72	M7.5	M7.4	4404A-7V	M7	
	15/16				4411-2I	M7	
	Dec. 7/8				4496-4V	M7:	
	8/9				4498-7V	M7:	
	8/9				4499-2V	M7	*
	10/11	11.33	M6.9	M6.8	4505-2I	M7	*
	10/11	11.33	M6.8	M6.9			
	Jan. 2/3	10.63	M6.4	M6.5	4510-5I	M6	
	3/4				4717-2V	M6:	
	3/4				4717-4V	$M6^+$	
RT Sgr	Oct.12/13	8.28	M5.2	M4.4			
	13/14				4270-4I	M5:	
RU Sgr	Oct.13/14				4270-2I	M7:	
	14/15	12.10	M6.8	M6.6			
	Nov.12/13	12.28	M7.3	M7.1			

TABLE IV. (continued)

STAR	DATE	V	S(V-R)	S(R-I)	PLATE-CAMP V: Visual I: Infrared	S	NOTE
T Scl	Oct.10/11	10.91	M5.5	M5.3			
	11/12	10.97	M5.6	M5.3			
	12/13				4268-2I	$M5^+$	
	14/15	11.24	M5.7	M5.4			
	Nov.12/13	12.84	M6.6	M6.4	4397-6V	$M6^+$	
	15/16	12.81	M6.6	M6.4			
	Dec. 7/8	12.28	M6.2	M6.1	4493-5V	M6	*
	10/11				4503-5I	M6	*
	Jan. 2/3				4509-2I	M6	*
	3/4	11.30	M5.9	M5.7	4714-7V	M6	*
R Tuc	Oct.10/11	9.92	M4.4	M4.8			
	14/15	10.01	M4.5	M4.8			
	Nov.14/15	10.58	M5.5	M5.6			
	Dec. 7/8	10.55	M6.1	M6.2			
	Jan. 2/3	12.42	M6.6	M6.4			
U Tuc	Oct.11/12	9.70	M4.8	M4.8			
	13/14	9.65	M4.8	M4.7			
	13/14	9.51	M4.7	--			
	Nov.14/15	8.71	M4.2	M4.4			
	Dec. 8/9	9.84	M5.5	M5.5			
	8/9	9.82	M5.4	M5.4			
	Jan. 3/4	11.44	M6.4	M6.3			
S Vol	Oct.12/13	13.31	M6.8	M6.9			
	Nov.14/15	13.58	M7.2	M7.3			
	Jan. 2/3	12.97	M7.0	M7.1			

($m_0 - M = 4.4$) and R Leo ($m_0 - M = 6.4$) (Robertson and Feast 1981), and they easily reach M7–M8 with $V - R > 4.5$. So, the sequence in the $(V - R, R - I)$ diagram can reach to M8 with large values of $V - R$ and $R - I$. It is possible to measure these values with the new high quantum efficiency photocathode in the near infrared (see Appendix).

The color indices are large and very sensitive to Me spectral subclass (Paper I). The colors in other regions ($\lambda\lambda$ 3700–5500 Å) are also good indicators of the spectral class and the depth of TiO bands for M-type stars and M Mira Variables (Maehara and Yamashita 1978). Towards high values of $(V - R)$ and $(R - I)$ the intensity of the TiO bands increases. The bands of TiO are one of the parameters that indicate the spectral subclass, according to the criteria of Keenan (1966), Seitter (1970, 1975), Keenan *et al.* (1974), Keenan and McNeil (1976), and Landi *et al.* (1977). Since in the calibration of Barnes (1973) the spectra were not obtained in his study, the analysis depended upon published spectral types. Furthermore, since the photometry and spectroscopy (of Barnes) were not simultaneous, the correlation is quite noisy.* However, Fig. 15 shows a correlation between the color indices and the spectral subclass in the Barnes' calibration for all Mira variables. Table VI includes a study of the relation for the present data. The inspection of this table shows that any relationship derived from groups of data are difficult to distinguish, if they exist. It is also clear from Fig. 15 that there is no apparent separation in the graph between stars with periods smaller or greater than 300 days. If there is any correlation it is very buried within the observational errors.

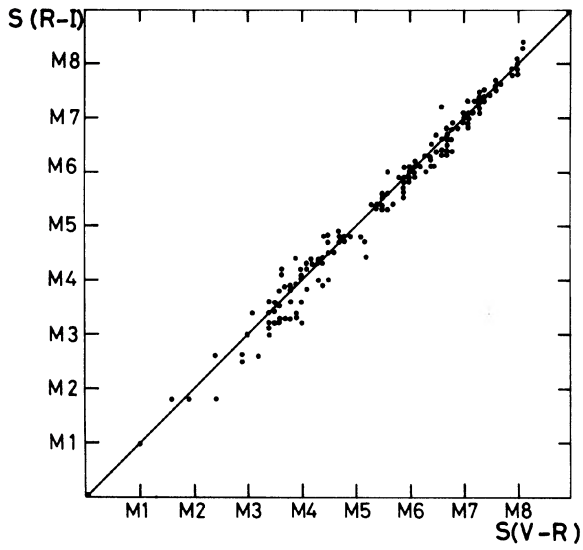

FIG. 14. Spectra $S(R - I)$ vs spectra $S(V - R)$. The 45° line is traced.

VII. CONCLUSIONS

The use of wideband photometry for determining the spectral subclass constitutes an essential tool in the study of red variable stars. Together with determining the photometric properties, it is possible to estimate the subclass to decimal places for any phase of the luminous cycle. The relationship between the spectrum and the color index of the Mira variables enables one to objectively estimate the subtype with an accuracy of 0.3 subtype, particularly for $S >$ M2, due to the operativeness of the process. The extension of the scale

*This was mentioned by Barnes (1973) himself on page 382.

TABLE V. Precision in the spectral subclassification.

S	$\sigma(S)_{V-R}$	$\sigma(S)_{R-I}$	$\sigma(S)$
M2	0.46	0.40	0.61
M3	0.25	0.20	0.32
M4	0.20	0.25	0.32
M5	0.27	0.07	0.27
M6	0.08	0.15	0.17
M7	0.11	0.08	0.14
M8	0.07	0.19	0.19
Mean	0.21	0.20	0.29

TABLE VI. Scale of spectral classification of Me Mira variables, using the color indices $V-R$ and $R-I$ and the calibrations of Johnson (1966), Barnes (1973), and present.

	Scale		Johnson (1966) red giants		Barnes (1963) $P<300$ days		Barnes (1963) $P>300$ days		Present $P<300$ days			Present $P>300$ days		
S	$V-R$	$R-I$	$V-R$	$R-I$	$V-R$	$R-I$	$V-R$	$R-I$	$V-R$	$R-I$	N	$V-R$	$R-I$	N
M0.0	1.07	0.82	1.23	0.94	1.57	1.53						1.07	0.83	1
M0.5	1.10	0.90												
M1.0	1.15	0.98	1.28	0.99										
M1.5	1.23	1.06							1.25	1.11	1	1.23	1.11	1
M2.0	1.26	1.14	1.34	1.10	1.17	0.98	2.26	1.80	1.26	0.91	1			
M2.25	1.29	1.18												
M2.5	1.32	1.22			1.42	1.33			1.31	1.22	1			
M2.75	1.36	1.27							1.39	1.20	1			
M3.0	1.41	1.36	1.48	1.31	1.51	1.28			1.45	1.20	1	1.41	1.37	1
M3.25	1.46	1.45							1.47	1.41	2			
M3.5	1.53	1.54			1.57	1.39			1.56	1.48	8	1.50	1.49	1
M3.75	1.60	1.63							1.63	1.66	8			
M4.0	1.69	1.72	1.74	1.65	1.55	1.49	2.03	1.76	1.70	1.75	7			
M4.25	1.79	1.81							1.77	1.83	9			
M4.5	1.89	1.90			1.63	1.50			1.88	1.91	5			
M4.75	2.01	1.99							2.04	2.00	6	2.02	1.98	4
M5.0	2.15	2.08	2.18	1.96	1.70	1.58	2.40	2.12	2.27	1.97	1	2.27	1.86	1
M5.25	2.30	2.17							2.32	2.23	1	2.34	2.24	1
M5.5	2.46	2.26			2.05	1.87	2.24	1.98	2.45	2.25	4			
M5.75	2.64	2.35							2.68	2.42	3			
M6.0	2.84	2.44	2.80	2.26	1.94	1.85	2.55	2.21	2.85	2.44	7	2.86	2.40	2
M6.25	3.06	2.53							3.16	2.51	8	3.07	2.55	2
M6.5	3.29	2.69			2.49	2.16	2.75	2.36	3.37	2.58	3	3.43	2.57	6
M6.75	3.54	2.71							3.58	2.71	7	3.70	2.75	2
M7.0	3.81	2.80					2.99	2.46	4.11	2.83	1	3.85	2.80	5
M7.25	4.10	2.89										4.15	2.84	4
M7.5	4.41	2.98							4.45	2.97	4	4.50	3.00	2
M7.75	4.74	3.07												
M8.0	5.09	3.16					3.40	2.77				5.06	3.12	3
M8.25	5.47	3.25										5.20	3.21	2

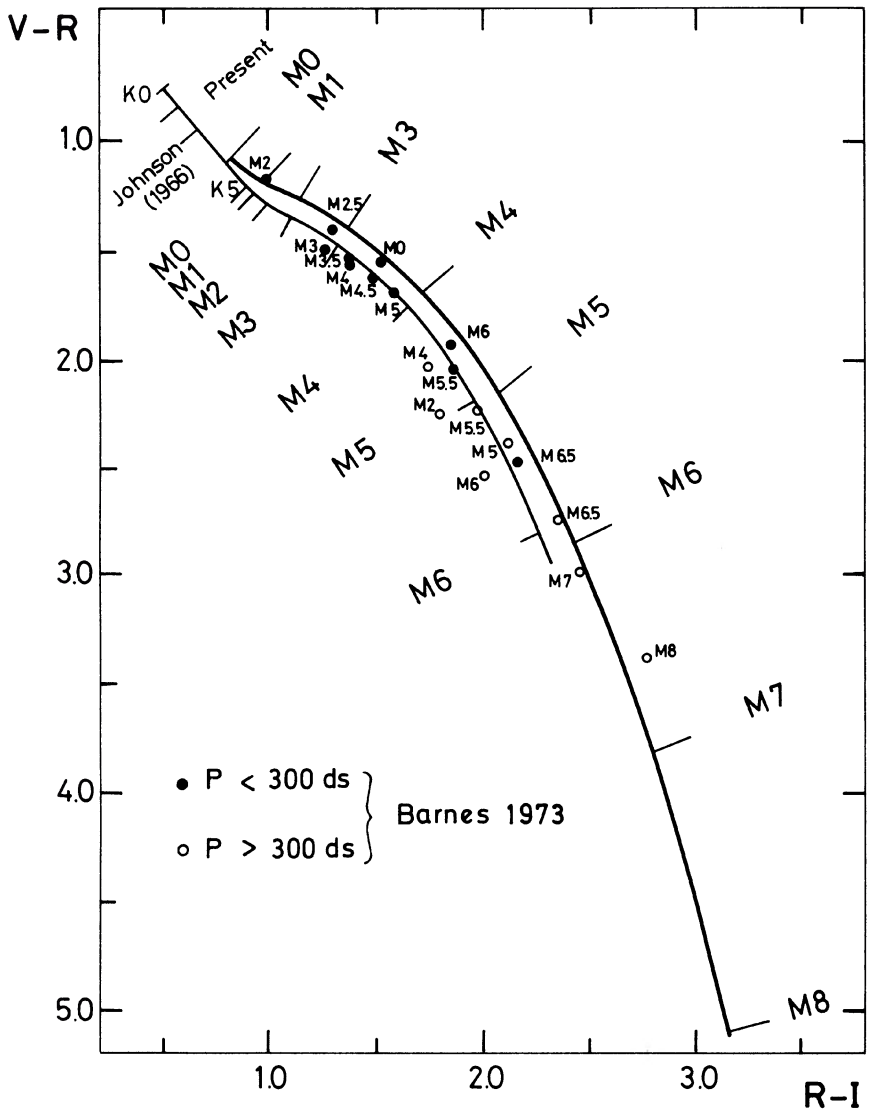

FIG. 15. Comparison of the present photometric calibration of Me spectral subclass with the calibrations of Johnson (1966) and Barnes (1973) in the two-color diagram ($V-R$, $R-I$).

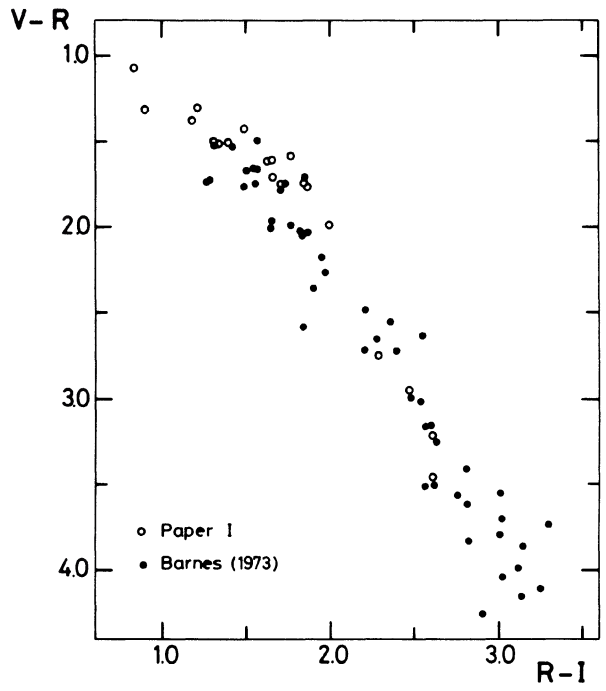

FIG. 16. Comparison for Mira variables of the photometry of Paper I with the photometry given by Barnes (1973) on the Johnson system. The $V-R$ and $R-I$ values are taken at maxima of the light curves.

up to the later M subtypes allows the classification up to the luminous minima, where most of the Miras are very faint.

Nevertheless, it is necessary to bear in mind that the precision is not sufficient for M0 and M1. To improve this, one should resort to phenomenological spectral classification. Fortunately, early M-type standard stars can be easily found. Another aspect to be considered carefully is that the scale must be applied to normal Miras. The stars whch have peculiar M spectra and/or emission lines, as in the case of R Aqr, which produces negative $U-B$ color indices, can produce an incorrect classification of the spectral type.

This work has been done under contract of the Academic Vice-Presidency, Research Division of the Catholic University of Chile, Proposal N^0. 12/82R. I thank my assistant-student, Mr. Rodrigo Montero, who helped me in obtaining spectrographic plates during the initial stages of the research.

APPENDIX

Table II of Paper I shows that the results for standard stars compare well with the results of Moffet and Barnes (1979a, b) and of Johnson (1966) on the Johnson system. The absence of M late standard stars may be indicating that the transformation from the natural system to the Johnson standard system is not trustworthy for stars as red as Miras. Moreover, in Paper I it is shown that the photometry was instrumentally realized on the Kron system, but, indeed, this photometry was transformed to the Johnson system.

To demonstrate explicitly that the data of Miras are on the Johnson system, the maxima of the Miras obtained by Barnes (1973) (on the Johnson system) are compared in Fig. 16 with the maxima found in Paper I for all Miras. The focus of the points in diagram ($V-R, R-I$) of both photometries is coincident. The dispersion of the values of Barnes is due to the low quantum efficiency of the ITT FW118 photomultiplier (S.1.). On the other hand, the high quantum efficiency of the RCA 31034 photocathode allows us to obtain large values of $V-R$ and $R-I$ for Miras at minimum, but with less dispersion.

REFERENCES

Barnes, T. G. (1973). Astrophys. J. Suppl. **221**, 369.
Bessell, M. S. (1976). Publ. Astron. Soc. Pac. **88**, 557.
Celis, S. L. (1975). Astron. Astrophys. Suppl. **22**, 9.
Celis, S. L. (1977). Astron. Astrophys. Suppl. **29**, 5.
Celis, S. L. (1978). Astron. Astrophys. **63**, 53.
Celis, S. L. (1979). Astron. Astrophys. **74**, 146.
Celis, S. L. (1980). Astron. Astrophys. **89**, 145.
Celis, S. L. (1981). Astron. Astrophys. **99**, 58.
Celis, S. L. (1982). Astron. J. **87**, 1791.
Deutsch, A. J., Wilson, O. C., and Keenan, P. C. (1969). Astrophys. J. **156**, 107.
Johnson, H. L. (1966). Annu. Rev. Astron. Astrophys. **4**, 193.
Johnson, H. M. (1981). Astrophys. J. **244**, 552.
Jones, D. H. P. (1978). *Spectral Classification of the Future*, IAU Colloquium No. 47, pp. 535–538.
Keenan, P. C. (1966). Astrophys. J. Suppl. XIII, **118**, 333.
Keenan, P. C., Garrison, R. F., and Deutsch, A. J. (1974). Astrophys. J. Suppl. **28**, 271.
Keenan, P. C., and McNeil, R. C. (1976). *An Atlas of Spectra of the Cooler Stars Types G, K, M, S* and *C* (The Ohio State University Press, Columbus, Ohio).
Kunkel, W. E., and Rydgren, A. E. (1979). Astron. J. **84**, 633.
Landi, J., Jaschek, M., and Jaschek, C. S. (1977). *An Atlas of Grating Stellar Spectra at Intermediate Dispersion* (Ed. Observatorio Astronómico de Córdoba, Argentina).
Maehara, H., and Yamashita, Y. (1978). Ann. Tokyo Astron. Obs., Second Ser., Vol. XVII, No. 2, 93.
Merril, P. W. (1940). *Spectra of Long Period Variable Stars* (University of Chicago Press), p. 82.
Moffet, T. J., and Barnes, T. G. (1979a). Publ. Astron. Soc. Pac, **91**, 180.
Moffet, T. J., and Barnes, T. G. (1979b). Astron. J. **84**, 627.
Rautela, B. S., and Joshi, S. C. (1979). Bull. Astron. Soc. India **7**, 43.
Robertson, B. S. C., and Feast, M. W. (1981). Mon. Not. R. Astron. Soc. **96**, 111.
Seitter, W. C. (1970). *Atlas for Objective Prism Spectra, Bonner Spectral Atlas I* (Ferd Dunnler, Bonn, West Germany).
Seitter, W. C. (1975). *Atlas for Objective Prism Spectra, Bonner Spectral Atlas II* (Ferd Dunnler, Bonn, West Germany).
Smak, J. (1964). Astrophys. J. Suppl. Vol. IX, No. 89, 141.
Smak, J., and Wing, R. F. (1979). Acta Astron. **29**, 187.
Sopka, R. J., Herbig, G., Kafatos, M., and Michalitsanos, A. G. (1982). Astrophys. J. Lett. **258**, L35.
Wallerstein, G., and Greenstein, J. L. (1980). Publ. Astron. Soc. Pac. **92**, 275.
Wing, R. F., and Yorka, S. B. (1978). *Spectral Classification of the Future*, IAU Colloquium No. 47, pp. 510–534.
Zuckerman, B. (1980). Annu. Rev. Astron. Astrophys. **18**, 263.